

# Transport coefficients in finite volume Polyakov–Nambu–Jona-Lasinio model

Kinkar Saha<sup>1</sup>, Sabyasachi Ghosh<sup>2</sup>, Sudipa Upadhyaya<sup>3,4</sup>, Soumitra Maity<sup>3,4</sup>

<sup>1</sup>*Department of Physics, University of Calcutta, 92, A. P. C. Road, Kolkata - 700009, India*

<sup>2</sup>*Indian Institute of Technology Bhilai, GEC Campus, Sejbahar, Raipur-492015, Chhattisgarh, India*

<sup>3</sup>*Center for Astroparticle Physics & Space Science, Block-EN,  
Sector-V, Salt Lake, Kolkata 700091, West Bengal, India and*

<sup>4</sup>*Department of Physics, Bose Institute, 93/1, A. P. C. Road, Kolkata 700009, West Bengal, India*

Finite size consideration of matter significantly affects transport coefficients like shear viscosity, bulk viscosity, electrical conductivity, which we have investigated here in the framework of the Polyakov–Nambu–Jona-Lasinio model. Owing to the basic quantum mechanics, a non-zero lower momentum cut-off is implemented in momentum integrations, used in the expressions of constituent quark masses and transport coefficients. When the system size decreases, the values of these transport coefficients are enhanced in low temperature range. At high temperature domain, shear viscosity and electrical conductivity become independent of system sizes. Whereas, bulk viscosity, which is associated with scale violating quantities of the system, faces some non-trivial size dependence in this regime. In the phenomenological direction, our microscopic estimations can also be linked with the macroscopic outcome, based on dissipative hydrodynamical simulation.

PACS numbers: 12.38.Mh, 25.75.-q, 25.75.Nq, 11.10.Wx, 51.20+d, 51.30+i

## I. INTRODUCTION

The experiment of relativistic heavy ion collider (RHIC) has created a nearly perfect fluid [1–3], whose shear viscosity to entropy density ( $\eta/s$ ) ratio is so small that it almost reaches the lower bound ( $\eta/s = 1/4\pi$ ) [4]. In the high temperature domain however, the theoretical calculations using perturbative methods surprisingly do not lead to such small value of  $\eta/s$ . There it behaves as weakly interacting gas, having relatively large value (10–20 times larger than lower bound) [5]. To resolve this discrepancy between experimental and theoretical values, different alternative calculations, based on effective QCD models [6–14] and hadronic models [15–24] have been studied in recent times. Some estimations are also done from the direction of transport simulations [25–28] and Lattice QCD calculations [29, 30]. Other transport coefficients like bulk viscosity ( $\zeta$ ) [6–8, 12–14, 17, 22–24, 31–49], electrical conductivity ( $\sigma$ ) [8, 50–66] of this QCD medium have also become matter of contemporary interest. From these earlier research, we get a gross summary about the temperature dependence of these transport coefficients.  $\eta(T)$  and  $\sigma(T)$  decrease and increase in temperature domains of hadron and quark phases respectively, while  $\zeta(T)$  follows an opposite trend. So, near transition temperature, one can expect a maximum in  $\zeta(T)$  [6, 7, 37, 49] and minimum in  $\eta(T)$  [6, 7, 9–11, 13] and  $\sigma(T)$  [57].

These analysis were carried out for infinite size systems. Effects of finiteness in system volumes have not however been considered which we are studying in this work. We know that the lower bound of shear viscosity to entropy density ratio ( $\eta/s$ ) is basically lowest possible quantum fluctuation of fluid, which can never vanish, even in the infinite coupling limit [4]. However, in this infinite coupling limit, we can think about a classical fluid, whose  $\eta/s \rightarrow 0$ . On the other hand,  $\eta/s$  of RHIC matter

is surprisingly close to its quantum lower bound, which indicates that the matter is very sensitive to the quantum fluctuations. Hence other possible quantum effect like finite size may be important to be considered. There is a long list of Refs. [67–97], where finite size effect on different physical quantities have been investigated. From experimental point of view as well, the produced fireball might have a finite system volume, depending on the size of the colliding nuclei, the center of mass energy and centrality of the collision. Significances of these issues raise immediate question on its impact over the transport coefficients of a system. In this manuscript, we intend to explore the same in a qualitative manner. For this initial work, we do so by implementing a lower momentum cut-off following the same line of studies as in [92]. Our studies have been carried out within the realm of Polyakov–Nambu–Jona-Lasinio (PNJL) model incorporating upto six quark type of interactions. This finite volume effect on transport coefficients is recently investigated in HRG model by Samanta et al. [98] and Sarkar et al. [99], which is valid for hadronic temperature domain only. Here we have explored this fact in PNJL model, which can well describe the thermodynamics of QCD medium for entire temperature domain, which contain quark and hadron both phases. This model also additionally contains the finite volume effect of quark condensate, for which a major change in transport coefficients is observed.

The article is organized as follows. Next section has covered the finite system size picture of PNJL model and then a brief formalism part of transport coefficients. Then our numerical outputs are analyzed in the result section and at last, we summarize our studies.

## II. THE MODEL FRAMEWORK

The framework that we shall be working with is that of 2+1 flavor PNJL model [100–108]. This model entwines two very basic features of QCD viz. chiral symmetry and its spontaneous breaking and confinement physics. The quark dynamics is incorporated in the NJL part through multi-quark interaction terms. Here we shall consider upto six-quark type of interactions. The gluon dynamics on the other hand, is taken care of through a background field representing Polyakov loop dynamics. There has been a considerable progress made in this direction in order to understand properly the strongly interacting system under this framework [8, 11, 49, 89, 90, 109–124].

The Polyakov loop potential [125] is expressed as,

$$\frac{\mathcal{U}[\Phi, \bar{\Phi}, T]}{T^4} = \frac{\mathcal{U}[\Phi, \bar{\Phi}, T]}{T^4} - \kappa \ln(J[\Phi, \bar{\Phi}]) \quad (1)$$

where, the second term on the right hand side is the Vander-monde term [106] reflecting the effect of SU(3) Haar measure.  $\mathcal{U}[\Phi, \bar{\Phi}, T]$  is the Landau-Ginzburg type potential chosen to be of the form,

$$\frac{\mathcal{U}[\Phi, \bar{\Phi}, T]}{T^4} = -\frac{b_2(T)}{2}\bar{\Phi}\Phi - \frac{b_3}{6}(\Phi^3 + \bar{\Phi}^3) + \frac{b_4}{4}(\Phi\bar{\Phi})^2 \quad (2)$$

The coefficients  $b_3$  and  $b_4$  are kept constant, whereas the temperature dependence is included in  $b_2$  with a form,

$$b_2(T) = a_0 + a_1\left(\frac{T_0}{T}\right) + a_2\left(\frac{T_0}{T}\right)^2 + a_3\left(\frac{T_0}{T}\right)^3 \quad (3)$$

All the associated parameters are set [125] through few physical constraints and the rest by fitting with available results from Lattice QCD. The set of parameters that we have chosen for present purpose can be found in [92].

For the quark dynamics, we shall use similar framework of NJL model except replacing with co-variant derivative in the kinetic part of the Lagrangian in presence of Polyakov loop. Under 2+1-flavor consideration with upto six-quark type of interactions, the Lagrangian gets modified as is given in [125]. As a result of dynamical breaking of chiral symmetry in the NJL model, the chiral condensate  $\langle\bar{\Psi}\Psi\rangle$  acquires non-zero vacuum expectation values. The constituent mass as a consequence is given by,

$$M_f = m_f - g_S\sigma_f + g_D\sigma_{f+1}\sigma_{f+2} \quad (4)$$

where  $\sigma_f \equiv \langle\bar{\Psi}_f\Psi_f\rangle$  represents the chiral condensate. If  $\sigma_f = \sigma_u$ , then  $\sigma_{f+1} = \sigma_d$  and  $\sigma_{f+2} = \sigma_s$  and in cyclic order.

Now in order to implement the effect of finite system sizes, one is ideally supposed to choose the proper boundary conditions : periodic for bosons and anti-periodic for fermions. This in effect leads to a sum of infinite extent over discretized momentum values,  $p_i = \frac{\pi n_i}{R}$ ,  $R$  being the dimension of cubical volume.  $n_i$  are positive integers with  $i=x,y,z$ . This would then imply an infra-red

cut-off  $p_{min} = \frac{\pi}{R} = \lambda(\text{say})$ . Ideally the surface and curvature effects should be taken care of as well. However, this being the very first case study in this direction, we are mostly interested in the qualitative changes of the transport coefficients under finite system size consideration. To obtain that, we incorporate few simplifications. The infinite sum over discrete momentum values will be replaced by integration over continuum momentum variation, albeit with the infra-red cut-off. Alongside, we are not going to use any amendments in the mean-field values due to finite system sizes. This in effect implies that the system volume,  $V$  will be regarded as a parameter just like temperature,  $T$  and chemical potential,  $\mu$  on the same footing. Parametrization will be the same as for zero  $T$ , zero  $\mu$  and infinite  $V$ . Any variation therefore occurring due to any of these parameters will be reflected in  $\sigma_f$ ,  $\Phi$  etc. and through them in meson spectra.

With these simplifications, the thermodynamic potential thereafter takes the form,

$$\begin{aligned} \Omega = & \mathcal{U}(\Phi[A], \bar{\Phi}[A], T) + 2g_S \sum_{f=u,d,s} \sigma_f^2 - \frac{g_D}{2} \sigma_u \sigma_d \sigma_s \\ & - 6 \sum_f \int_{\lambda}^{\Lambda} \frac{d^3 p}{(2\pi)^3} E_{p_f} \Theta(\Lambda - |\vec{p}|) - 2 \sum_f T \int_{\lambda}^{\infty} \frac{d^3 p}{(2\pi)^3} \\ & \ln \left[ 1 + 3 \left( \Phi + \bar{\Phi} e^{\frac{-(E_{p_f} - \mu_f)}{T}} \right) e^{\frac{-(E_{p_f} - \mu_f)}{T}} + e^{\frac{-3(E_{p_f} - \mu_f)}{T}} \right] \\ & - 2 \sum_f T \int_{\lambda}^{\infty} \frac{d^3 p}{(2\pi)^3} \\ & \ln \left[ 1 + 3 \left( \Phi + \bar{\Phi} e^{\frac{-(E_{p_f} + \mu_f)}{T}} \right) e^{\frac{-(E_{p_f} + \mu_f)}{T}} + e^{\frac{-3(E_{p_f} + \mu_f)}{T}} \right] \end{aligned} \quad (5)$$

where, each term bears its usual significance, which can be found in [125].

## III. TRANSPORT COEFFICIENTS

Green-Kubo relation [126, 127] connects transport coefficients like shear viscosity  $\eta$ , bulk viscosity  $\zeta$  and electrical conductivity  $\sigma$  to their respective thermal fluctuation or correlation functions -  $\langle\pi^{ij}(x)\pi_{ij}(0)\rangle_{\beta}$ ,  $\langle\mathcal{P}(x)\mathcal{P}(0)\rangle_{\beta}$  and  $\langle J^i(x)J_i(0)\rangle_{\beta}$ , where  $\langle\cdot\rangle_{\beta}$  stands for thermal average. The operators  $\pi_{ij}$  and  $\mathcal{P}$  can be obtained from energy-momentum tensor  $T^{\mu\nu}$  as,

$$\begin{aligned} \pi^{ij} & \equiv T^{ij} - g^{ij} T_k^k / 3, \\ \mathcal{P} & \equiv -T_k^k / 3 - c_s^2 T^{00} \end{aligned} \quad (6)$$

where  $c_s$  is speed of sound in the medium. The operator  $J^i$  is the electromagnetic current of medium constituents. The transport coefficients in momentum space can be written explicitly in spectral representations as,

$$\eta = \frac{1}{20} \lim_{q_0, \vec{q} \rightarrow 0} \frac{\int d^4 x e^{iq \cdot x} \langle [\pi^{ij}(x), \pi_{ij}(0)] \rangle_{\beta}}{q_0}$$

$$\zeta = \frac{1}{2} \lim_{q_0, \vec{q} \rightarrow 0} \frac{\int d^4 x e^{iq \cdot x} \langle [\mathcal{P}(x), \mathcal{P}(0)] \rangle_\beta}{q_0},$$

$$\sigma = \frac{1}{6} \lim_{q_0, \vec{q} \rightarrow 0} \frac{\int d^4 x e^{iq \cdot x} \langle [J^i(x), J_i(0)] \rangle_\beta}{q_0} \quad (7)$$

Our aim of this work is to calculate these transport coefficients of quark matter under the framework of PNJL model and to notice their changes because of the finite size consideration of medium. As we know that the mathematical expressions of transport coefficients, calculated from relaxation time approximation (RTA) in kinetic theory approach and the one-loop diagram in quasi-particle Kubo approach are exactly same, let us start with the standard expressions of  $\eta$  [17, 18, 128],  $\zeta$  [12, 17] and  $\sigma$  [17, 63, 129] given by,

$$\eta = \frac{g}{15T} \int \frac{d^3 \vec{k}}{(2\pi)^3} \tau_Q \left( \frac{\vec{k}^2}{\omega_Q} \right)^2 [f_Q^+(1 - f_Q^+) + f_Q^-(1 - f_Q^-)] ; \quad (8)$$

$$\zeta = \frac{g}{T} \int \frac{d^3 \vec{k}}{(2\pi)^3} \tau_Q \left\{ \left( \frac{1}{3} - c_s^2 \right) \vec{k}^2 - c_s^2 m_Q^2 - c_s^2 m_Q T \frac{dM_Q}{dT} \right\}^2 [f_Q^+(1 - f_Q^+) + f_Q^-(1 - f_Q^-)] ; \quad (9)$$

$$\sigma = \frac{6\tilde{e}_Q^2}{3T} \int \frac{d^3 \vec{k}}{(2\pi)^3} \tau_Q \left( \frac{\vec{k}}{\omega_Q} \right)^2 [f_Q^+(1 - f_Q^+) + f_Q^-(1 - f_Q^-)] , \quad (10)$$

where  $g = 2 \times 2 \times 3$  is degeneracy factor of quark,  $f_Q^\pm$  are the modified Fermi-Dirac (FD) distribution functions of quarks and anti-quarks respectively in presence of Polyakov loop.  $\omega_Q = \{\vec{k}^2 + m_Q^2\}^{1/2}$  is the single quasi-particle energy and

$$\tilde{e}_Q^2 = \left\{ \left( +\frac{2}{3} \right)^2 + \left( -\frac{1}{3} \right)^2 \right\} e^2 . \quad (11)$$

#### IV. NUMERICAL RESULTS AND DISCUSSIONS

Let us first take a glance at the expressions of transport coefficients, given in Eqs. (8), (9) and (10). Replacing the  $\vec{k} = 0$  by  $\vec{k} = \pi/R$  in the lower limit of the integrations, we have adopted the effect of finite size of quark matter, having the dimension  $R$ . Along with this, there is another place in Eqs. (8), (9) and (10), where the finite size effect enters. This is the integrand part of transport coefficients, which depends on the constituent quark mass and thus changes due to consideration of finite size of

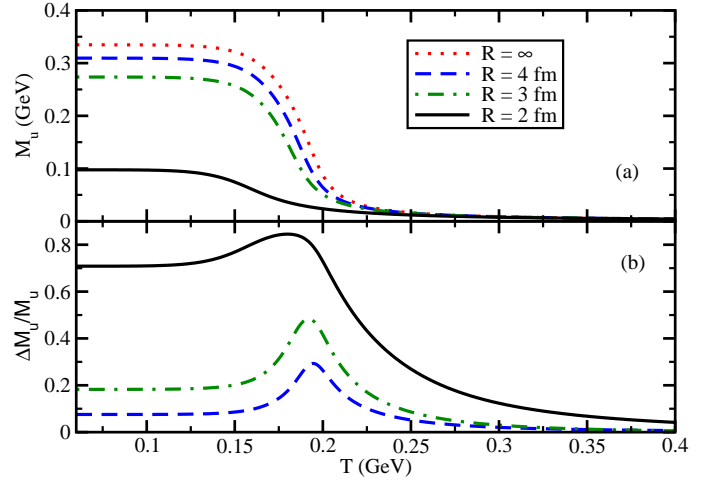


FIG. 1: (Color online) (a)  $T$  dependence of  $u$  (or  $d$ ) quark mass for  $R = \infty$  (red dotted line), 4 fm (blue dashed line), 3 fm (green dash-dotted line) and 2 fm (black solid line). (b) Change of the  $u$  (or  $d$ ) quark mass for the same finite size parameters with respect to the quark mass for  $R = \infty$ .

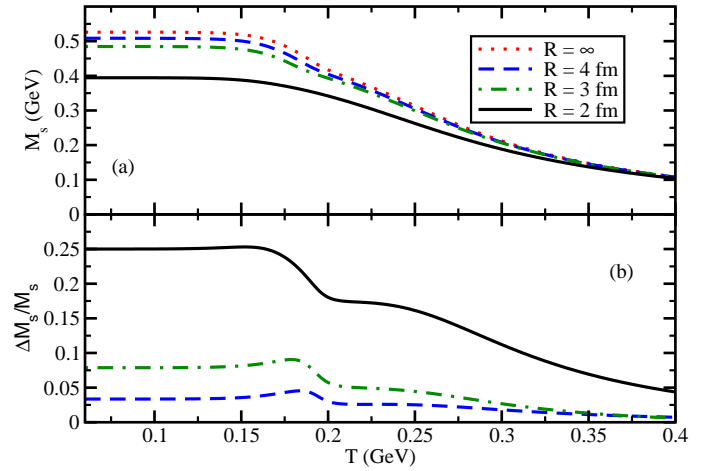


FIG. 2: (Color online) Same as Fig. (1) for strange quark.

quark matter. So there are two sources from where finite size effect will modify our numerical estimations of transport coefficients.

Before analyzing the numerical outputs, let us discuss about the limitations of our present formalism. In finite temperature quantum field theory, we have to introduce the imaginary time parameter, which can vary from  $\tau = 0$  to  $\tau = -i\beta$ . This finite time restriction makes the energy component discretized via Matsubara prescription (imaginary time formalism). Similarly, restriction of finite size or length ( $L$ ) makes the momentum component discretized i.e. the four momentum variables  $(k_0, \vec{k})$  will be discretized as  $k_0 \rightarrow \omega_n = \frac{2\pi}{\beta}(n + 1/2)$  and  $\vec{k} \rightarrow \vec{k}_n = \frac{2\pi}{L}(n + 1/2)$ , where  $n = 0, \pm 1, \pm 2, \dots$  because of

finite temperature  $T = 1/\beta$  and length  $L$  [85]. Following analytic continuation technique, the discrete sum of energies can be transformed to its continuous integration. For three momentum component, their discrete sum is roughly assumed as continuous integration, starting from the lower momentum cutoff. This simplified picture of finite size effect by implementing lower momentum cut-off is justified in Refs. [94, 95]. It is nicely demonstrated in Fig. (1) of Ref. [94]. Along with the discretization of momentum, surface and curvature effects may appear in the finite size picture [77] but we don't consider these effects in the present work for simplicity.

Let us now start our numerical discussion from the size dependency of constituent quark mass, which is shown in Figs. (1) and (2). As can be seen from Eq. (4), the temperature dependent condensates determine the temperature dependence of constituent quark masses, which are plotted by red dotted lines in Figs. 1(a) and 2(a) for u and s quarks. These are the results of  $M_u(T)$  and  $M_s(T)$  when we have not considered any finite size effect. We have marked this result by  $R = \infty$ . Now, introducing finite size consideration in gap equation (Eq. (4)), we get the curves - blue dashed line, green dash-dotted line and black solid line for  $R = 4$  fm, 3 fm, 2 fm respectively in Figs. 1(a) and 2(a). To zoom in the changes of masses due to finite size effect, we have defined,

$$\frac{\Delta M_{u,s}}{M_{u,s}} = \frac{M_{u,s} - M_{u,s}(R)}{M_{u,s}}, \quad (12)$$

where  $M_{u,s}(R)$  are u, s quark masses for the medium with dimension  $R$  and  $M_{u,s}$  for  $R = \infty$ . These  $\frac{\Delta M_{u,s}}{M_{u,s}}$  are plotted in Figs. 1(b) and 2(b) for  $R = 4$  fm, 3 fm and 2 fm. We see that  $\frac{\Delta M_{u,s}}{M_{u,s}}$  increases as  $R$  decreases, shows a mild peak before melting down at high temperature. The peaks mainly appear because of faster melting rates of  $M(R=\infty)$  compared to the rest. The vanishing nature of  $\frac{\Delta M_{u,s}}{M_{u,s}}$  at high  $T$  limit is expected because of gradual restoration of chiral symmetry in that regime for any system size. So, one may safely ignore the finite size effect of quark gluon plasma (QGP), produced in heavy ion experiments, when it remains very hot, far above transition temperature,  $T_c$ . The finite size effect of QCD medium becomes important near  $T_c$  and its non-perturbative (hadronic) temperature domain. This general feature of finite size effect is observed for various quantities, discussed later.

Now, using the expression of  $M_{u,s}(T, R)$  and lower momentum cutoff  $\vec{k} = \pi/R$  in Eq. (8), we can generate  $\eta(T)$  for different values of  $R$ . Following same definition, given in Eq. (12), we have defined  $\Delta\eta/\eta$ , which are plotted in Fig. 3(a). The negative values of  $\Delta\eta/\eta$  below  $T = 200$  MeV indicate that shear viscosity gets enhanced because of finite size effect. In one side,  $\eta$  should be decreased because of lower momentum cutoff in Eq. (8), while on other side, reduction of constituent quark mass for finite  $R$  will act on the integrand part of Eq. (8) to enhance the values of  $\eta$ . Latter source dominates over the former

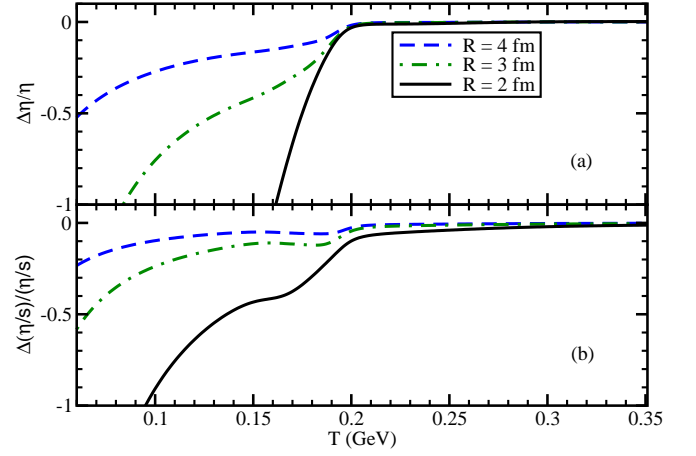


FIG. 3: (Color online) Difference between the results of finite and infinite  $R$  for the quantities - shear viscosity  $\eta$  (a) and shear viscosity to entropy density ratio  $\eta/s$  (b).

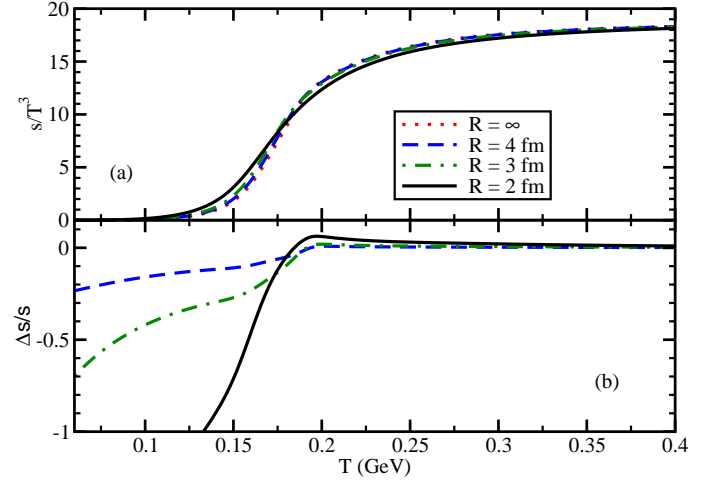


FIG. 4: (Color online) (a)  $T$  dependence of entropy density, normalized by  $T^3$  for different values of  $R$ . (b) Difference between finite and infinite matter results for entropy density.

one, therefore, a net enhancement of  $\eta(T < 200$  MeV) is observed in our results. Next, to discuss the finite size effect on  $\eta/s$ , shown in Fig. 3(b), let us focus on entropy density  $s$ , obtained from the thermodynamical potential  $\Omega$ . Figs. 4(a) and (b) show the  $T$  dependences of  $s/T^3$  and  $\Delta s/s$  for different values of  $R$ . When this finite size effect of  $s$  at low  $T$  enters into the quantity  $\eta/s$ , a less amount of enhancement of  $\eta/s$  has been found with respect to the enhancement of  $\eta$ . For example, at  $T = 170$  MeV and  $R = 2$  fm in Fig. (3), we see that 70% enhancement in  $\eta$  shrinks to 40% enhancement in  $\eta/s$ . Also, for vanishing chemical potential, we observe only cross-over transitions, which is true for all  $R$ . So no discontinuity in  $\eta$  or  $\eta/s$  is observed. However, with decreasing  $R$ ,  $T_c$  is supposed to decrease [92] and that is visible in



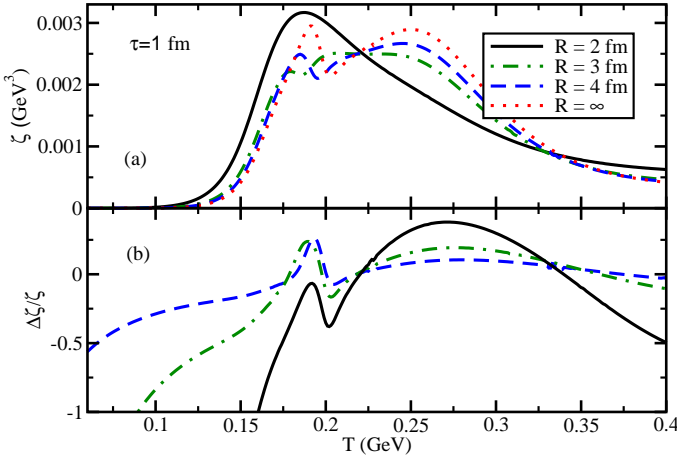


FIG. 5: (Color online) (a)  $\zeta(T)$  for  $R = \infty$  (red dotted line), 4 fm (blue dashed line), 3 fm (green dash-dotted line) and 2 fm (black solid line). (b) Difference between finite and infinite matter results for  $\zeta$ .

Fig. 3(b). The locations of slight bending there, grossly representing the transition region, shift towards lower  $T$  with decrease in  $R$ .

Let us come to the next transport coefficient - bulk viscosity  $\zeta$ , which is a very interesting quantity because of its relation with conformal symmetry of the system. Compared to Eq. (8) for  $\eta$ ,  $\zeta$  in Eq. (9) contains additionally a conformal breaking term

$$\left\{ \left( \frac{1}{3} - c_s^2 \right) \vec{k}^2 - c_s^2 \left( M_Q^2 + M_Q T \frac{dM_Q}{dT} \right) \right\}^2, \quad (13)$$

which vanishes in the limits of  $c_s^2 \rightarrow 1/3$  and  $M_Q \rightarrow 0$ . The QCD matter at high temperature can achieve these limits, where it behaves as a scale independent or conformally symmetric system. It can alternatively be realized from the vanishing values of  $\zeta$  for this QCD matter at high temperature. Relating to this fact, our bulk viscosity estimation in PNJL model is trying to measure indirectly the breaking of this conformal symmetric nature of QCD matter in both quark and hadronic domain. In this context, the present investigation has tried to explore the finite system size effect on this breaking of conformal symmetry by studying the  $R$  dependence of  $\zeta$ . For a constant value of relaxation time ( $\tau = 1/\Gamma = 1$  fm), we have estimated  $\zeta(T)$  for  $R = \infty$  (red dotted line), 4 fm (blue dashed line), 3 fm (green dash-dotted line) and 2 fm (black solid line), which are drawn in Fig. 5(a). We see double peak-like structures in  $\zeta$ , which are also observed in other earlier calculations [12, 48]. These double peak-like structures start diluting as we decrease system sizes and for  $R = 2$  fm such nature disappears, indicating some non-trivial contributions from strange sectors. As we know, with decreasing system sizes, the constituent masses acquire smaller values in the low temperature domain, thereby tending towards restoring the chiral sym-

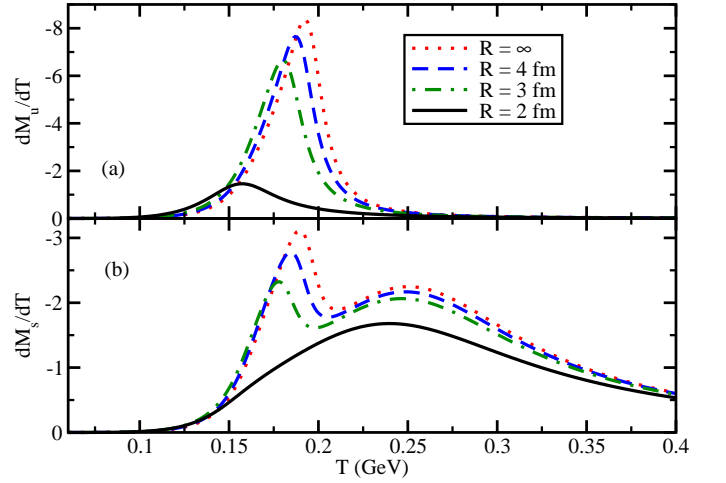


FIG. 6: (Color online) (a)  $\frac{dM_u}{dT}$  and (b)  $\frac{dM_s}{dT}$  for  $R = \infty$  (red dotted line), 4 fm (blue dashed line), 3 fm (green dash-dotted line) and 2 fm (black solid line).

metry over the entire temperature window.

To understand these facts, we have to focus on the conformal breaking term, given in Eq. (13), where  $dM_{u,s}/dT$  is one of the main controlling parameters, which is shown in Fig. (6). We observe that the peak position of  $dM_{u,d}/dT$  in Fig. 6(a), which represents the transition temperature ( $T_c$ ) of chiral phase, shifts towards lower temperature as  $R$  decreases. The peak strength of  $dM_{u,d}/dT$  also decreases when  $R$  decreases. If we focus on  $\zeta(T)$  for light ( $u$  and  $d$ ) quark matter only, then it follows exactly same pattern of  $dM_{u,d}/dT$  i.e. peak strength of  $\zeta(T)$  reduces and its peak position shifts towards lower  $T$  as  $R$  decreases. The complex two peak structure comes into picture when we add  $s$  quark contribution, which participates partially in chiral phase transition. Apart from the expected peak near  $T_c$ ,  $dM_s/dT$  exhibits an additional peak at higher temperature and therefore, we get two peak structure in  $\zeta(T)$  for 2 + 1 flavor quark matter. The first peak in  $dM_s/dT$  is little sharper than the second one. Both are reduced when  $R$  decreases but at  $R = 2$  fm, the first peak almost vanishes. So, only second peak survives in  $dM_s/dT$  at  $R = 2$  fm and its magnitude is interestingly comparable to the corresponding magnitude of  $dM_{u,d}/dT$ . As a net effect, we get one broadened (not sharp) peak at some intermediate location between the peak positions of  $dM_{u,d}/dT$  and  $dM_s/dT$  for  $R = 2$  fm.

Apart from the term  $dM_{u,d,s}/dT$ , another component of conformal breaking is  $c_s^2$ , which is shown in Fig. 7(a). As  $c_s^2 = s/\{T ds/dT\}$ , for vanishing quark chemical potential the  $R$  dependence of  $c_s^2$  is quite similar to the  $R$  dependence of  $s$ , shown in Fig. 4(a). The changes in  $c_s^2$  are shown more precisely in Fig. 7 by plotting  $\Delta c_s^2/c_s^2$  vs.  $T$  for different values of  $R$ . So, from  $R$  dependences of  $dM_{u,d,s}/dT$  and  $c_s^2$ , given in Figs. (6) and (7), we can grossly understand the qualitative nature of  $\zeta(T, R)$ ,

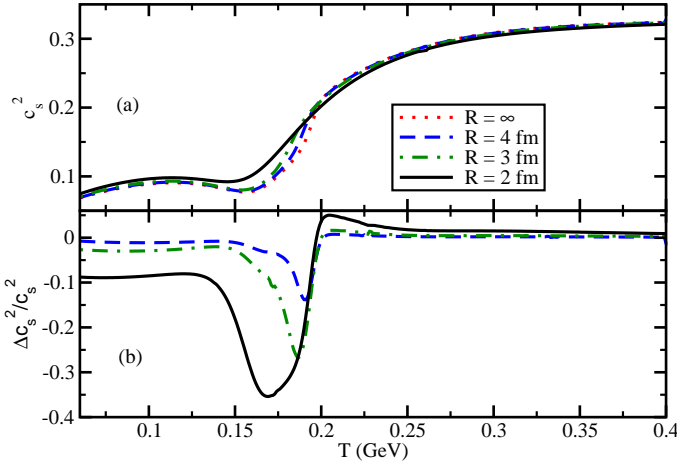


FIG. 7: (Color online) Same as Fig. (5) for square of speed of sound  $c_s^2$ .

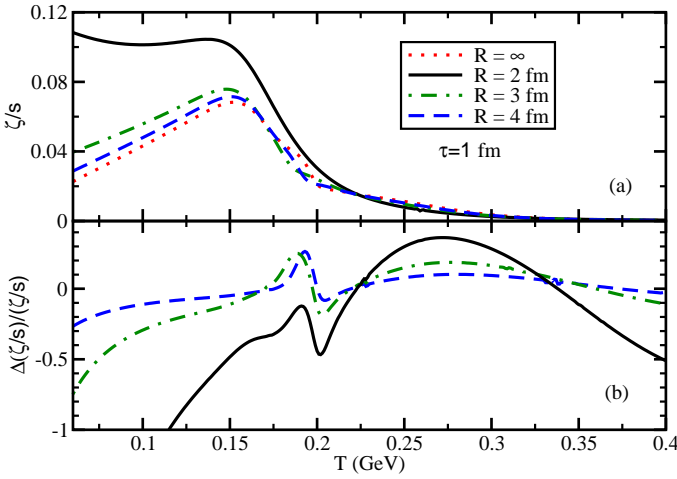


FIG. 8: (Color online) Same as Fig. (5) for bulk viscosity to entropy density ratio  $\zeta/s$ .

given in Fig. 5(b). The changes of  $\zeta$  are explored in Fig. 5(b), where we notice that  $\Delta\zeta/\zeta$  remains non-zero at high temperature zone, unlike  $\Delta\eta/\eta$  or others. This is because of strange quark contribution. Unlike  $dM_{u,d}/dT$  curves in Fig. 6(a),  $dM_s/dT$  curves for different values of  $R$ , shown in Fig. 6(b), do not merge at high temperature zone ( $T = 0.170 - 0.400$  GeV). If we restrict our outcome to  $u$  and  $d$  quarks, then we will get a vanishing  $\Delta\zeta/\zeta$  at that high temperature region.

Now, normalizing the bulk viscosity by the entropy density, we have plotted  $\zeta/s$  and its change  $\Delta(\zeta/s)/(\zeta/s)$  for different values of  $R$  in Figs. 8(a) and (b) respectively. Though  $\zeta$  at low temperature limit almost tends to zero but  $\zeta/s$  at that limit becomes finite because of their comparable magnitudes. Interestingly, the second (mild) peak of  $\zeta$  almost disappears in  $\zeta/s$  because  $s(T)$  at high  $T$  domain is strongly dominant and increases rapidly

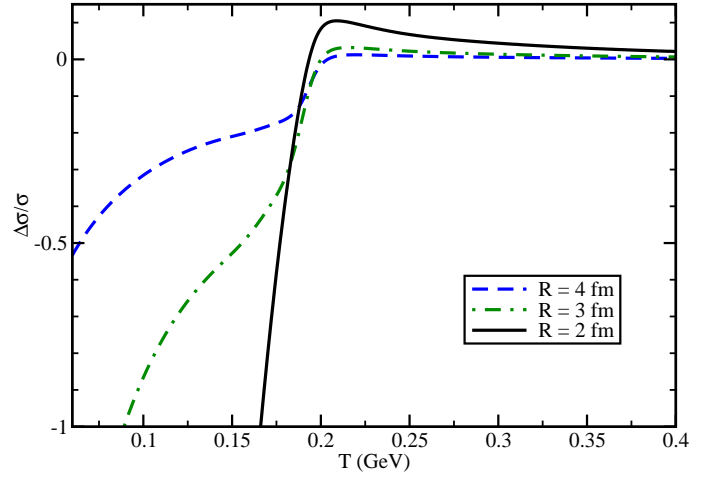


FIG. 9: (Color online) Difference between finite and infinite matter results for electrical conductivity  $\sigma$  for different values of  $R$ .

with respect to  $\zeta(T)$ . Comparing Figs. 5(b) and 8(b), we notice that the changes of  $\zeta$  and  $\zeta/s$  due to finite size are approximately similar.

Next, let us come to the electrical conductivity  $\sigma$  of quark matter, whose expression is given in Eq. (10). Using this expression, we have generated  $\sigma(T)$  with and without finite size effect and then following our earlier technique, we define  $\Delta\sigma/\sigma$ , which is plotted in Fig. (9) for different values of  $R$ . As the expressions of  $\eta$  and  $\sigma$  are quite similar, therefore, one can see a similarity between the results of Fig. 3(b) and Fig. (9). However, one should notice that the integrand of  $\sigma$  is  $\vec{k}^2$  times smaller than that of  $\eta$ , which is the main reason of quantitative difference between  $\Delta\sigma/\sigma$  and  $\Delta\eta/\eta$ . For example, at  $T = 0.170$  GeV  $R = 2$  fm,  $\Delta\sigma/\sigma = -80\%$  but  $\Delta\eta/\eta = -70\%$ . One more interesting difference between  $\Delta\sigma/\sigma$  and  $\Delta\eta/\eta$  is that at high  $T$  range,  $\sigma(R)$  reduces with respect to  $\sigma(R = \infty)$ . For example, at  $T = 0.200$  GeV  $R = 2$  fm,  $\Delta\sigma/\sigma = +8\%$  but  $\Delta\eta/\eta = -4\%$ . This clearly happens because of the absence of a  $\vec{k}^2$  factor in  $\sigma$  compared to that in  $\eta$ .

#### A. Comparison with NJL results

Without Polyakov loop extension, we have also generated the results for NJL models, where the straight forward Fermi-Dirac distribution function will describe the statistical probability of quarks in medium. So, the finite size effect will enter here through the modification of quark condensates or quark masses only. Whereas in PNJL model, Polyakov loop field  $\Phi$  will also have finite size effect along with the condensates. Unlike condensate, the Polyakov loop in present formalism don't carry any momentum integration so direct implementation of finite size effect by introducing the lower momentum cut-

off is not possible for this case. However, one can do it by following some different potential, which carry momentum integration [130, 131]. In present framework, Polyakov loop field faces an indirect finite size effect. In Fig.10(a), we see the field variable  $\Phi$  face a mild change when we jump from  $R = \infty$  to 2 fm, while a drastic change is noticed in quark mass  $M_u$  for the same transition in  $R$ . Fig. 10(b) shows the  $T$  dependent quark mass  $M_u$  at  $R = \infty$  and  $R = 2$  fm from PNJL model (dotted and solid lines) and NJL model (dash-dotted and dashed lines). We notice that condensate starts to melt down at lower temperature in NJL model than with respect to PNJL model but the strengths of their condensate at  $T = 0$  is exactly same. This observation is true for both infinite and finite matter but when one transits from infinite to finite matter picture for any model (NJL or PNJL), its vacuum condensate strength is abruptly reduced. When we see the curves of Fig. 11(a), which are basically the temperature derivatives of curves in Fig. 10(b), we can visualize the phase transition more clearly. We know that peak position of  $dM_u/dT$  for NJL model gives us the chiral transition temperature while, PNJL model contain collectively both chiral and deconfinement transition. In our present model, deconfinement transition takes place at higher temperature than the chiral transition temperature, therefore, the peak position of  $dM_u/dT$  for PNJL model shifts towards a higher temperature than the same for NJL model. When one transits from infinite to finite matter case for any model, the peak position shifts towards lower temperature. It means that transition temperature decreases by reducing the size of the medium, which is also noticed in earlier Refs. [89, 97]. Next, Fig. 11(b) reveals similar kind of peak shifting for strange quark but it contain an additional hump structure in higher temperature, which is well discussed in earlier section. These peak shifting will make direct impact on bulk viscosity.

Following similar patterns of Figs. 10 and 11, the entropy density  $s$  and speed of sound  $c_s$  are shown in Figs.12(a) and (b) respectively. In low temperature range, both quantities are enhanced when one goes from PNJL to NJL model as well as from infinite to finite matter case. At high temperature, an opposite behavior is observed. Finally, we come to the transport coefficients -  $\eta$ ,  $\zeta$  and  $\sigma$  in NJL and PNJL model for  $R = \infty$  and 2 fm, which are shown in Figs. 13(a), (b) and (c) respectively. We can grossly conclude that both  $\eta$  and  $\sigma$  are enhanced during the transition from PNJL to NJL model as well as from infinite to finite matter case. Although, all of the curves merge at high temperature region. This is expected because the thermal distribution functions of NJL and PNJL model become same at high temperature range. Again, the thermodynamic probability of quarks at lower momentum is negligible for this high temperature domain, so impact of lower momentum cutoff for finite size consideration of medium, will also be negligible. Therefore the curves for  $R = \infty$  and  $R = 2$  fm both merge at high temperature domain. For bulk viscosity,

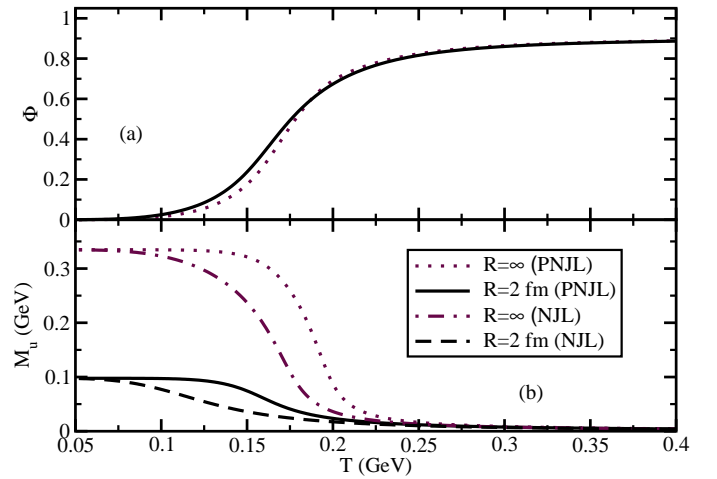


FIG. 10: (Color online) (a) :  $T$  dependence of field  $\Phi$  at  $R = \infty$  (dotted line) and  $R = 2$  fm (solid line). (b) : Quark mass  $M_u(T)$  at  $R = \infty$  and  $R = 2$  fm from PNJL model (dotted and solid lines) and NJL model (dash-dotted and dashed lines).

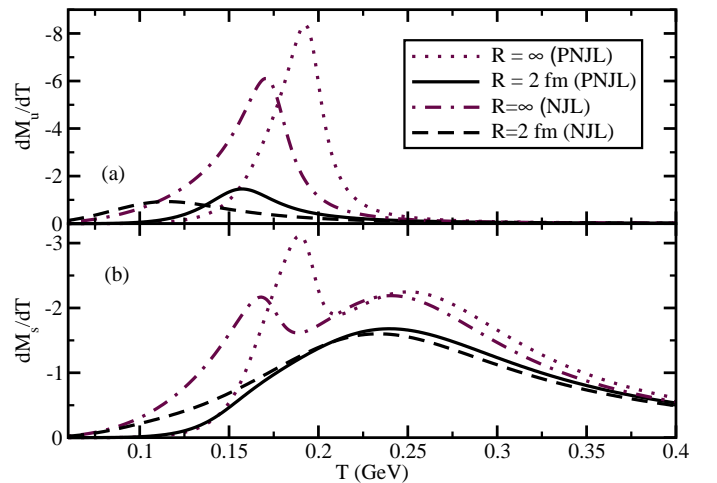


FIG. 11: (Color online) Same as Fig. 10(b), the  $T$  dependence of  $dM_u/dT$  (a) and  $dM_s/dT$  (b) are shown.

$dM_u/dT$  and  $dM_s/dT$  of Figs. 11(a) and (b) will collectively build its profile, which is little complex in structure. In earlier section, for PNJL model, we have already analyzed how two peak structure of  $\zeta$  is converted to one broadened peak structure. Same event is happening for NJL model also but its positions of peaks in  $T$  axis are only different.

## B. Phenomenological significance

Now let us see the connection or application of our studies in heavy ion phenomenology. The expanding

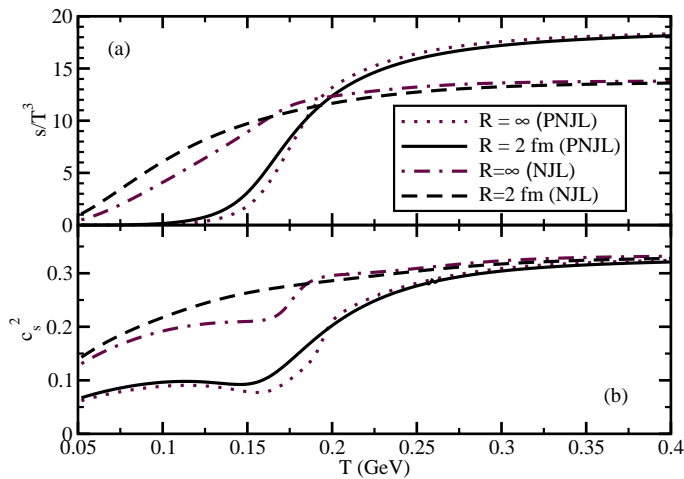


FIG. 12: (Color online) Following the same pattern of earlier figure, the comparison between NJL and PNJL model results for entropy density  $s(T)$  and speed of sound  $c_s(T)$ .

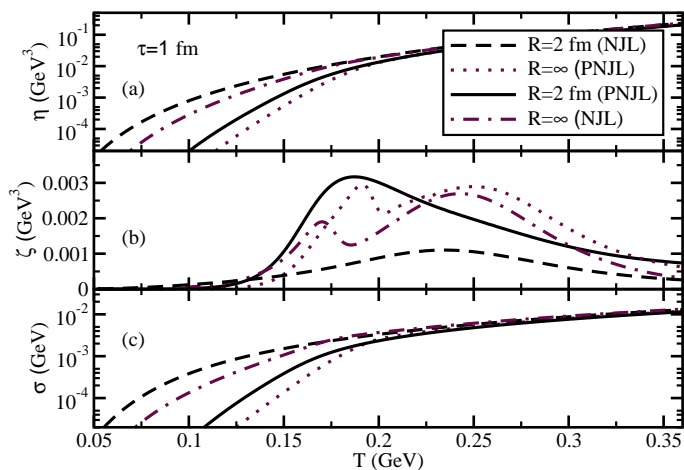


FIG. 13: (Color online) Following the same pattern of earlier figure, the comparison between NJL and PNJL model results for shear viscosity  $\eta$ , bulk viscosity  $\zeta$  and electrical conductivity  $\sigma$ .

medium, created in heavy ion collision experiments, can be well described by dissipative hydrodynamic simulations, where the transport coefficients like shear and bulk viscosities are implemented as input parameters. When the medium expands, its volume increases and temperature decreases with time. At certain temperature, called freeze-out temperature, the medium loses its many body identity. In experiment, only this freeze-out size of the medium can be measured. However, before the freeze-out point, the size of the expanding medium can be smaller than its freeze-out size. Our present investigation reveals that the values of  $\eta/s$  and  $\zeta/s$  can be changed for different system sizes, which are less than 6-7 fm (approx). So one should consider size dependent (along with temperature

dependent)  $\eta/s$  and  $\zeta/s$  during the complete evolution.

In most central collision, the freeze-out size is quite large ( $\sim 7 - 8$  fm) but in non-central collision, it can be smaller. So, at different centrality, one can expect different values of transport coefficients. In Ref. [3], the centrality dependence of invariant yield and elliptic flow of charged hadrons as a function of transverse momentum has been investigated. They have matched the experimental data of PHENIX Collaboration [132, 133] by taking different guess values of  $\eta/s$  in the hydrodynamical simulation and they found the experimental data prefers higher values of  $\eta/s$  as we go from central to peripheral collisions. The same indication is found in our present work. When one goes from central to peripheral collisions, which means from higher to lower system sizes, our estimated values of  $\eta/s$  are enhanced. From microscopic direction, our understanding is that the quantum effect due to finite size of the system is responsible for enhancing the values of  $\eta/s$ .

## V. SUMMARY AND PERSPECTIVES

As a first attempt to investigate the qualitative changes brought about by finite size effect on transport coefficients of quark matter, we have adopted here a simple idea of taking non-zero lower momentum cut-off under the framework of PNJL model. The temperature dependences of constituent quark masses, obtained from the gap equation, have been modified and they get diminished as size of the system decreases. When these size dependent quark masses are plugged in the integrands of different transport coefficients, then some enhancements in their values are found. Whereas, the expressions of transport coefficients contain momentum integrations as well, whose non-zero lower limit contributes additionally to the effects of medium size which basically decreases as we decrease the size. So, there will be a competition between these two sources of finite size, which will determine the net change in the values of transport coefficients. In low temperature range, shear viscosity and electrical conductivity increase as system size is reduced. The size effect disappears at high temperature range, as chiral symmetry gets restored there for any system size. The bulk viscosity, which basically measures the scale violation of the medium, has a non-trivial link with the system size. The rate of change of constituent quark mass with respect to temperature and speed of sound are two quantities responsible for that.

We have also analyzed the same studies for NJL model case just to understand the transition between NJL and PNJL models. We have noticed that the values of transport coefficients are grossly enhanced when we transit from PNJL to NJL model as well as from infinite matter to finite matter. This enhancement mostly occurs in low temperature domain and almost vanishes at high temperature domain.

In phenomenological direction, our microscopic calcu-



lations say that  $\eta/s$  of the medium increases when one goes from central to peripheral collisions. Similar conclusion is also found from the macroscopic direction, where dissipative hydrodynamical simulation describes the expanding medium by taking  $\eta/s$  as an input parameter.

In order to see the qualitative changes in transport coefficients for finite system size consideration, we have taken constant value of relaxation time in this present work. However, involved calculations of relaxation time at finite temperature as well as system sizes incorporating different interaction channels might lead us to more realistic scenario. We intend to address the issue in our

future project.

**Acknowledgment:** SG is partially supported from University Grant Commission (UGC) Dr. D. S. Kothari Post Doctoral Fellowship (India) under grant No. F.4-2/2006 (BSR)/PH/15-16/0060. KS acknowledges the partial financial supports by DST-SERB Ramanujan fellowship of Tamal Mukherjee under project no. SB/S2/RJN-29/2013 and DST-SERB NPDF under Fellowship ref. no. PDF/2017/002399. SU and SM thank DST and CSIR for financial support. SG acknowledges WHEPP-2017 for getting some fruitful discussions.

- 
- [1] P. Romatschke and U. Romatschke, Phys. Rev. Lett. **99**, 172301 (2007).
  - [2] M. Luzum and P. Romatschke, Phys. Rev. C **78**, 034915 (2008).
  - [3] V. Roy, A. K. Chaudhuri and B. Mohanty, Phys. Rev. C **86**, 014902 (2012).
  - [4] P. Kovtun, D. T. Son, and O. A. Starinets, Phys. Rev. Lett. **94**, 111601 (2005).
  - [5] P. B. Arnold, G. D. Moore, and L. G. Yaffe, J. High Energy Phys. **11**, 001 (2000); 05, 051 (2003).
  - [6] P. Chakraborty and J. I. Kapusta, Phys. Rev. C **83**, 014906 (2011).
  - [7] C. Sasaki, K. Redlich, Nucl. Phys. A **832**, 62 (2010).
  - [8] R. Marty, E. Bratkovskaya, W. Cassing, J. Aichelin, H. Berrehrhah, Phys. Rev. C **88**, 045204 (2013).
  - [9] S. Ghosh, A. Lahiri, S. Majumder, R. Ray, S. K. Ghosh, Phys. Rev. C **88**, 068201 (2013).
  - [10] R. Lang, W. Weise Eur. Phys. J. A **50**, 63 (2014); R. Lang, N. Kaiser, W. Weise, Eur. Phys. J. A **51**, 127 (2015).
  - [11] S. K. Ghosh, S. Raha, R. Ray, K. Saha, S. Upadhaya, Phys. Rev. D **91**, 054005 (2015).
  - [12] S. Ghosh, T. C. Peixoto, V. Roy, F. E. Serna, and G. Krein, Phys. Rev. C **93**, 045205 (2016).
  - [13] P. Deb, G. Kadam, H. Mishra, Phys. Rev. D **94**, 094002 (2016).
  - [14] A. N. Tawfik, A. M. Diab, M.T. Hussein, Int.J.Mod.Phys. A31, 1650175 (2016); arXiv:1610.06041 [nucl-th].
  - [15] K. Itakura, O. Morimatsu, and H. Otomo, Phys. Rev. D **77**, 014014 (2008).
  - [16] A. Dobado and S.N. Santalla, Phys. Rev. D **65**, 096011 (2002); A. Dobado and F. J. Llanes-Estrada, Phys. Rev. D **69**, 116004 (2004).
  - [17] D. Fernandez-Fraile and A. Gomez Nicola, Eur. Phys. J. C **62**, 37 (2009).
  - [18] R. Lang, N. Kaiser and W. Weise Eur. Phys. J. A **48**, 109 (2012).
  - [19] S. Mitra, S. Ghosh, and S. Sarkar Phys. Rev. C **85**, 064917 (2012).
  - [20] S. Ghosh, G. Krein, S. Sarkar, Phys. Rev. C **89**, 045201 (2014); S. Ghosh, Phys. Rev. C **90** 025202 (2014); S. Ghosh, Braz. J. Phys. **45**, 687 (2015).
  - [21] M. I. Gorenstein, M. Hauer, O. N. Moroz, Phys. Rev. C **77**, 024911 (2008).
  - [22] G. P. Kadam and H. Mishra, Nucl. Phys. A **934**, 133 (2015).
  - [23] G. P. Kadam and H. Mishra, Phys. Rev. C **92**, no. 3, 035203 (2015).
  - [24] J. Noronha-Hostler, J. Noronha, C. Greiner, Phys. Rev. Lett. **103**, 172302 (2009).
  - [25] N. Demir and S.A. Bass Phys. Rev. Lett. **102**, 172302 (2009).
  - [26] A. Muronga, Phys. Rev. C **69**, 044901 (2004).
  - [27] S. Plumari, A. Puglisi, F. Scardina, and V. Greco, Phys. Rev. C **86**, 054902 (2012).
  - [28] S. Pal, Phys. Lett. B **684**, 211 (2010).
  - [29] H. B. Meyer, Phys. Rev. D **76**, 101701 (2007); Phys. Rev. D **82**, 054504 (2010).
  - [30] N. Astrakhantsev, V. Braguta, A. Kotov, J. High Energy Phys. **1704** (2017) 101; J. High Energy Phys. **1509** (2015) 082.
  - [31] K. Paech and S. Pratt, Phys. Rev. C **74**, 014901 (2006).
  - [32] S. Gavin, Nucl. Phys. A, **435**, 826 (1985).
  - [33] P. Arnold, C. Dogan, G. D. Moore, Phys. Rev. D **74**, 085021 (2006).
  - [34] M. Prakash, M. Prakash, R. Venugopalan, and G. Welke, Phys. Rep. **227**, 321 (1993).
  - [35] D. Kharzeev, K. Tuchin, JHEP **0809**, 093 (2008).
  - [36] F. Karsch, D. Kharzeev, K. Tuchin, Phys. Lett. B **663**, 217 (2008).
  - [37] X. Shi-Song, G. Pan-Pan, Z. Le, H. De-Fu, Chin. Phys. C **38**, 054101 (2014).
  - [38] C. Sasaki, K. Redlich, Phys. Rev. C **79**, 055207 (2009).
  - [39] V. Chandra, Phys. Rev. D **86**, 114008 (2012); Phys. Rev. D **84**, 094025 (2011).
  - [40] S. K. Das, J. Alam Phys.Rev. D **83**, 114011 (2011).
  - [41] S. Mitra and S. Sarkar, Phys. Rev. D **87**, 094026 (2013).
  - [42] G. P. Kadam and H. Mishra, Phys. Rev. C **93**, no. 2, 025205 (2016).
  - [43] G. Sarwar, S. Chatterjee and J. e. Alam, J. Phys. G **44**, no. 5, 055101 (2017).
  - [44] D. Fernandez-Fraile and A. Gomez Nicola, Phys. Rev. Lett. **102**, 121601 (2009).
  - [45] S. Ghosh, S. Chatterjee, B. Mohanty Phys. Rev. C **94**, 045208 (2016).
  - [46] H. B. Meyer, Phys. Rev. Lett. **100**, 162001 (2008).
  - [47] A. Dobado, F.J.Llane-Estrada, J. Torres Rincon, Phys. Lett. B **702**, 43 (2011).
  - [48] A. Dobado, J. Torres Rincon, Phys. Rev. D **86**, 074021 (2012).
  - [49] K. Saha, S. Upadhaya and S. Ghosh, Mod. Phys. Lett.

- A **32**, no. 05, 1750018 (2016).
- [50] H.T. Ding, A. Francis, O. Kaczmarek, F. Karsch, E. Laermann, and W. Soeldner, Phys. Rev. D **83**, 034504 (2011).
- [51] G. Aarts, C. Allton, J. Foley, S. Hands, and S. Kim, Phys. Rev. Lett. **99**, 022002 (2007).
- [52] P. V. Buividovich, M. N. Chernodub, D. E. Kharzeev, T. Kalaydzhyan, E. V. Luschevskaya, and M. I. Polikarpov, Phys. Rev. Lett. **105**, 132001 (2010).
- [53] Y. Burnier and M. Laine, Eur. Phys. J. C **72**, 1902 (2012).
- [54] S. Gupta, Phys. Lett. B **597**, 57 (2004).
- [55] B. B. Brandt, A. Francis, H. B. Meyer, and H. Wittig, J. High Energy Phys. **03**, 100 (2013).
- [56] A. Amato, G. Aarts, C. Allton, P. Giudice, S. Hands, J.I. Skullerud, Phys. Rev. Lett. **111**, 172001 (2013).
- [57] W. Cassing, O. Linnyk, T. Steinert, and V. Ozvenchuk, Phys. Rev. Lett. **110**, 182301 (2013).
- [58] A. Puglisi, S. Plumari, V. Greco, Phys. Rev. D **90**, 114009 (2014); J. Phys. Conf. Ser. **612**, 012057 (2015); Phys. Lett. B **751**, 326 (2015).
- [59] M. Greif, I. Bouras, Z. Xu, C. Greiner, Phys. Rev. D **90**, 094014 (2014); J. Phys. Conf. Ser. **612**, 012056 (2015).
- [60] P. K. Srivastava, L. Thakur, B. K. Patra, Phys. Rev. C **91**, 044903 (2015).
- [61] S. I. Finazzo, J. Noronha Phys. Rev. D **89**, 106008 (2014).
- [62] C. Lee, I. Zahed, Phys. Rev. C **90**, 025204 (2014).
- [63] D. Fernandez-Fraile and A. Gomez Nicola, Phys. Rev. D **73**, 045025 (2006).
- [64] M. Greif, C. Greiner, G.S. Denicol, Phys. Rev. D **93**, 096012 (2016).
- [65] S. Ghosh, F. E. Serna, G. Krein, *in progress*
- [66] S. Ghosh, Phys. Rev. D **95**, no. 3, 036018 (2017).
- [67] A. E. Ferdinand and M. E. Fisher, Phys. Rev. **185**, 832 (1969).
- [68] M. E. Fisher and M. N. Barber, Phys. Rev. Lett. **28**, 1516 (1972).
- [69] M. Luscher, Commun. Math. Phys. **104**, 177 (1986).
- [70] H. T. Elze and W. Greiner, Phys. Lett. B **179**, 385 (1986).
- [71] J. Gasser and H. Leutwyler, Phys. Lett. B **188**, 477 (1987).
- [72] C. Spieles, H. Stoecker and C. Greiner, Phys. Rev. C **57**, 908 (1998).
- [73] A. Gopie and M. C. Ogilvie, Phys. Rev. D **59**, 034009 (1999).
- [74] O. Kiriya and A. Hosaka, Phys. Rev. D **67**, 085010 (2003).
- [75] C. S. Fischer and M. R. Pennington, Phys. Rev. D **73**, 034029 (2006).
- [76] L. M. Abreu, M. Gomes and A. J. da Silva, Phys. Lett. B **642**, 551 (2006).
- [77] G. y. Shao, L. Chang, Y. x. Liu and X. l. Wang, Phys. Rev. D **73**, 076003 (2006).
- [78] S. Yasui and A. Hosaka, Phys. Rev. D **74**, 054036 (2006).
- [79] A. Bazavov and B. A. Berg, Phys. Rev. D **76**, 014502 (2007).
- [80] L. F. Palhares, E. S. Fraga and T. Kodama, J. Phys. G **38**, 085101 (2011).
- [81] J. Luecker, C. S. Fischer and R. Williams, Phys. Rev. D **81**, 094005 (2010).
- [82] J. Braun, B. Klein and P. Piasecki, Eur. Phys. J. C **71**, 1576 (2011).
- [83] E. S. Fraga, L. F. Palhares and P. Sorensen, Phys. Rev. C **84**, 011903 (2011).
- [84] J. Braun, B. Klein and B. J. Schaefer, Phys. Lett. B **713**, 216 (2012).
- [85] L. M. Abreu, A. P. C. Malbouisson and J. M. C. Malbouisson, Phys. Rev. D **83**, 025001 (2011).
- [86] L. M. Abreu, A. P. C. Malbouisson and J. M. C. Malbouisson, Phys. Rev. D **84**, 065036 (2011).
- [87] D. Ebert, T. G. Khunjua, K. G. Klimenko and V. C. Zhukovsky, Int. J. Mod. Phys. A **27**, 1250162 (2012).
- [88] F. C. Khanna, A. P. C. Malbouisson, J. M. C. Malbouisson and A. E. Santana, Europhys. Lett. **97**, 11002 (2012).
- [89] A. Bhattacharyya, P. Deb, S. K. Ghosh, R. Ray and S. Sur, Phys. Rev. D **87**, no. 5, 054009 (2013).
- [90] A. Bhattacharyya, R. Ray and S. Sur, Phys. Rev. D **91**, no. 5, 051501 (R) (2015).
- [91] A. Bhattacharyya, R. Ray, S. Samanta and S. Sur, Phys. Rev. C **91**, no. 4, 041901 (R) (2015).
- [92] A. Bhattacharyya, S. K. Ghosh, R. Ray, K. Saha and S. Upadhyaya, Euro. phys. Lett. **116**, no. 5, 52001 (2016).
- [93] N. Magdy, M. Csand and R. A. Lacey, J. Phys. G **44**, no. 2, 025101 (2017).
- [94] K. Redlich and K. Zalewski, arXiv:1611.03746 [nucl-th].
- [95] F. Karsch, K. Morita, K. Redlich, Phys. Rev. C **93**, 034907 (2016).
- [96] H. j. Xu, Phys. Lett. B **765**, 188 (2017).
- [97] A. Bhattacharyya, S. K. Ghosh, R. Ray and S. Samanta, Europhys. Lett. **115**, no. 6, 62003 (2016).
- [98] S. Samanta, S. Ghosh, B. Mohanty, arXiv:1706.07709 [hep-ph].
- [99] N. Sarkar, P. Ghosh, arXiv:1711.08721 [hep-ph].
- [100] P. N. Meisinger and M. C. Ogilvie, Phys. Lett. B **379**, 163 (1996); Nucl. Phys. B (Proc. Suppl.) **47**, 519 (1996).
- [101] K. Fukushima, Phys. Lett. B **591**, 277 (2004).
- [102] C. Ratti, M. A. Thaler, and W. Weise, Phys. Rev. D **73**, 014019 (2006).
- [103] E. Megias, E. R. Arriola, and L. L. Salcedo, J. High Energy Phys. **01**, 073 (2006); Phys. Rev. D **74**, 114014 (2006); **74**, 065005 (2006).
- [104] S. k. Ghosh, T. K. Mukherjee, M. G. Mustafa, and R. Ray, Phys. Rev. D **73**, 114007 (2006).
- [105] S. Mukherjee, M. G. Mustafa, and R. Ray, Phys. Rev. D **75**, 094015 (2007).
- [106] S. k. Ghosh, T. K. Mukherjee, M. G. Mustafa, and R. Ray, Phys. Rev. D **77**, 094024 (2008).
- [107] H. -M. Tsai and B. Muller, J. Phys. G **36**, 075101 (2009).
- [108] E. Megias, E. R. Arriola, and L. L. Salcedo, Phys. Rev. Lett. **109**, 151601 (2012); Phys. Rev. D **89**, 076006 (2014).
- [109] H. Abuki and K. Fukushima, Phys. Lett. B **676**, 57 (2009).
- [110] H. Abuki, M. Ciminale, R. Gatto, and M. Ruggieri, Phys. Rev. D **79**, 034021 (2009).
- [111] J. K. Boomsma and D. Boer, Phys. Rev. D **80**, 034019 (2009).
- [112] A. Bhattacharyya, P. Deb, S. K. Ghosh, and R. Ray Phys. Rev. D **82**, 014021 (2010).
- [113] Y. Sakai, T. Sasaki, H. Kouno, and M. Yahiro, Phys. Rev. D **82**, 096007 (2010).
- [114] A. Bhattacharyya, P. Deb, A. Lahiri, and R. Ray Phys.

- Rev. D **82**, 114028 (2010); **83**, 014011 (2011).
- [115] A. Bhattacharyya, S. K. Ghosh, S. Majumder, and R. Ray, Phys. Rev. D **86**, 096006 (2012).
  - [116] A. Bhattacharyya, S. Das, S. K. Ghosh, S. Raha, R. Ray, K. Saha, and S. Upadhaya, arXiv:1212.6010.
  - [117] M. Dutra, O. Loureno, A. Delfino, T. Frederico, and M. Malheiro, Phys. Rev. D **88**, 114013 (2013).
  - [118] A. Bhattacharyya, S. K. Ghosh, A. Lahiri, S. Majumder, S. Raha, and R. Ray, Phys. Rev. C **89**, 064905 (2014).
  - [119] X. Xin, S. Qin and Y. -x. Liu, Phys. Rev. D **89**, 094012 (2014).
  - [120] C. A. Islam, R. Abir, M. G. Mustafa, S. K. Ghosh, and R. Ray, J. Phys. G **41**, 025001 (2014).
  - [121] S. K. Ghosh, A. Lahiri, S. Majumder, M. G. Mustafa, S. Raha, and R. Ray, Phys. Rev. D **90**, 054030 (2014).
  - [122] C. A. Islam, S. Majumder, N. Haque, and M. G. Mustafa, J. High. Ener. Phys. **1502**, 011 (2015).
  - [123] A. Bhattacharyya, S. K. Ghosh, S. Maity, S. Raha, R. Ray, K. Saha, and S. Upadhaya, Phys. Rev. D **95**, 054005 (2017).
  - [124] A. Bhattacharyya, S. K. Ghosh, S. Maity, S. Raha, R. Ray, K. Saha, S. Samanta, and S. Upadhaya, arXiv:1708.04549 [hep-ph].
  - [125] P. Deb, A. Bhattacharyya, S. Datta, and S. K. Ghosh, Phys. Rev. C **79**, 055208 (2009).
  - [126] D. N. Zubarev *Non-equilibrium statistical thermodynamics* (New York, Consultants Bureau, 1974).
  - [127] M. S. Green, J. Chem. Phys. **22**, 398 (1954); R. Kubo, J. Phys. Soc. Jpn. **12**, 570 (1957).
  - [128] S. Ghosh, Int. J. Mod. Phys. A **29**, 1450054 (2014).
  - [129] S. Ghosh, Phys. Rev. D **95**, 036018 (2017).
  - [130] P. N. Meisinger, T. R. Miller, and M. C. Ogilvie, Phys. Rev. D **65**, 034009 (2002).
  - [131] A. Dumitru, Y. Guo, Y. Hidaka, C. P. K. Altes, R. D. Pisarski Phys. Rev. D **83**, 034022, (2011).
  - [132] A. Adare et al. (PHENIX Collaboration), Phys. Rev. Lett. **105**, 062301 (2010).
  - [133] S. S. Adler et al. (PHENIX Collaboration), Phys. Rev. C **69**, 034910 (2004).